

**Environmental Security Technology Certification Program  
(ESTCP)**

**Final Report**

**Handheld Sensor for UXO Discrimination  
ESTCP Project 200108**



**T. H. Bell  
AETC Incorporated**

**August 12, 2004**

# CONTENTS

Acronyms .....	iii
Figures .....	iv
Tables .....	v
1. Introduction.....	1
1.1. Background.....	1
1.2. Objectives of the Demonstration .....	1
1.3. Regulatory Drivers.....	3
1.4. Stakeholder/End-User Issues .....	4
2. Technology Description.....	4
2.1. Technology Development and Application .....	4
2.2. Previous Testing of the Technology .....	10
2.3. Factors Affecting Cost and Performance.....	12
2.4. Advantages and Limitations of the Technology .....	12
3. Demonstration Design .....	14
3.1. Performance Objectives.....	14
3.2. Selecting Test Sites.....	14
3.3. Test Site History/Characteristics.....	15
3.4. Present Operations .....	18
3.5. Pre-Demonstration Testing and Analysis .....	18
3.6. Testing and Evaluation Plan .....	18
3.6.1. Demonstration Set-Up and Start-Up.....	18
3.6.2. Period of Operation.....	18
3.6.3. Area Characterized.....	18
3.6.4. Residuals Handling .....	18
3.6.5. Operating Parameters for the Technology .....	18
3.6.6. Experimental Design.....	19
3.6.7. Sampling Plan .....	21
3.6.8. Demobilization.....	21
4. Performance Assessment .....	21
4.1. Performance Criteria.....	21
4.2. Performance Confirmation Methods.....	22
4.3. Data Analysis, Interpretation and Evaluation .....	24
5. Cost Assessment .....	27
5.1. Cost Reporting .....	27

5.2.	Cost Analysis .....	29
6.	Implementation Issues .....	29
6.1.	Environmental Checklist.....	29
6.2.	Other Regulatory Issues.....	30
6.3.	End-User Issues .....	30
7.	References.....	30
8.	Points of Contact.....	31
APPENDIX A. Data Storage and Archiving Procedures .....		A1

## ACRONYMS

AEC	Army Environmental Center
APG	Aberdeen Proving Ground
ASCII	American Standard Code for Information Interchange
ATC	Aberdeen Test Center
BRAC	Base Realignment and Closure
CERCLA	Comprehensive Environmental Response, Compensation, and Liability Act
DoD	Department of Defense
EMI	Electromagnetic Induction
EOD	Explosive Ordnance Disposal
EPA	Environmental Protection Agency
ESTCP	Environmental Security Technology Certification Program
FUDS	Formerly Used Defense Site
HEAT	High Energy Anti-Tank
IDL	Interactive Data Language (Research Systems, Inc.)
ITRC	Interstate Technology Regulatory Council
PVC	Polyvinyl Chloride
QA	Quality Assurance
QC	Quality Control
RCRA	Resource Conservation and Recovery Act
RMS	Root Mean Square (standard deviation)
ROC	Receiver Operating Characteristic
SERDP	Strategic Environmental Research and Development Program
UXO	Unexploded Ordnance

## FIGURES

Figure 1. Electromagnetic induction and the EM61-HH sensor head. ....	5
Figure 2. Geonics EM61-HH (left) and setup for cued identification (center, right). ....	6
Figure 3. EM61-HH grid template.....	7
Figure 4. Ratio of EM61-HH signal at last time gate to signal at first time gate for thin walled scrap metal compared to UXO.....	8
Figure 5. Fit error (top) and beta (bottom) trajectories vs. focal depth for inversion of grid data over 2.75 inch rocket warhead in different orientations. ....	9
Figure 6. Standard inert ordnance items (left) and clutter from ATC (right). ....	10
Figure 7. Nonmetallic test stand for controlled testing the EM61-HH system.....	10
Figure 8. $\beta_s$ for ordnance and clutter determined from test stand and pit measurements. ....	11
Figure 9. GEM-3 handheld broadband EMI sensor.....	13
Figure 10. UXO Technology Demonstration Site at Aberdeen Test Center. ....	15
Figure 11. Layout of Calibration Lanes.....	16
Figure 12. Layout of Blind Test Grid. ....	17
Figure 13. User interface for inversion and target classification (see text for description).....	20
Figure 14. EM61-HH ROC from Blind Grid Scoring Report [7].....	24
Figure 15. Sample mean and standard deviation for first time gate data (left) and Histogram of the ratio of sample standard deviation to sample mean for signal level $>200$ mV (right)....	26
Figure 16. Scatter plot of dipole model fit error vs. mean signal (left) and histogram of the ratio of fit error to signal level (right). ....	27
Figure 17. Sample EM61-HH data file .....	A1

## **TABLES**

Table 1. Inert Ordnance Targets at the Aberdeen Test Site.....	2
Table 2. ATC Blind Grid Demonstration Performance Summary .....	14
Table 3. Period of Operation of the Demonstration at ATC.....	18
Table 4. Performance Criteria for Demonstration .....	22
Table 5. Expected Performance and Performance Confirmation Methods .....	22
Table 6. Complete Summary of Blind Grid Performance .....	23
Table 7. Noise levels for EM61-HH grids.....	26
Table 8. Standardized Blind Grid Demonstration Labor Costs. ....	28
Table 9. Summary of ATC Blind Grid Labor Costs.....	29
Table 10. Points of Contact.....	31

# **1. Introduction**

## **1.1. Background**

As a result of past military training and weapons-testing activities, UXO is present at sites designated for Base Realignment and Closure (BRAC) and at Formerly Used Defense Sites (FUDS). Current estimates indicate that over 11 million acres of land potentially contain UXO. Using current technologies, the cost of identifying and disposing of UXO in the United States is estimated to be in the billions of dollars. Current technology has shown improvements in our ability to detect sub-surface UXO but is unable to reliably discriminate UXO from other items that pose no risk. Current remediation approaches are labor intensive, slow, and expensive. The goal of this project is to demonstrate that, with the right post-processing of the sensor output, a simple, commercially available handheld sensor (Geonics EM61-HH metal detector) can be used to discriminate between buried UXO and subsurface clutter.

For several years now, with SERDP and ESTCP funding, AETC has been developing advanced processing techniques for discriminating between UXO and clutter using magnetic and electromagnetic induction (EMI) sensors. For EMI sensors, our approach [1] is based on estimating the magnetic polarizability tensor [2, 3] of an unknown buried object from data collected above the ground. The eigenvalues of the magnetic polarizability tensor are determined by the size and shape of the object, and can be used effectively in discriminating between UXO and clutter.

The basic idea is to collect data at a set of known positions over a target using the EM61-HH and its data recorder. After a number of targets have been interrogated in this manner, the data is downloaded to a notebook computer and fed into a program that determines the polarizability eigenvalues. A set of predetermined decision rules is then used to classify the target as either UXO or clutter. We have used this procedure successfully with precisely positioned array data and with data collected on a fixed grid.

## **1.2. Objectives of the Demonstration**

The objective of this project was to demonstrate the extent to which a simple, commercially available handheld sensor (Geonics EM61-HH) can be used to discriminate between buried UXO and clutter. The handheld sensor is used in a cued identification mode – data are collected directly above a flagged target and inverted to estimate target parameters for use in target classification and discrimination. The actual demonstration consisted of two stages or parts: (a) Interrogate the targets in the Blind Test Grid of the Aberdeen Proving Ground Standardized

UXO Technology Demonstration Site and (b) Analyze the data collected and derive target dig lists ordered by grid-center signal strength and by dig priority based on target classification. The demonstration was conducted at the Aberdeen Proving Ground Standardized UXO Technology Demonstration Site. Inert munitions and clutter items are positioned in various orientations and depths in the ground at the site. The ordnance targets emplaced in the test areas at the site are listed in Table 1. Standard targets are members of a set of specific ordnance items that have identical properties to all other items in the set (caliber, configuration, size, weight, aspect ratio, material, filler, magnetic remnance, and nomenclature). Nonstandard targets are ordnance items having properties that differ from those in the set of standardized targets.

**Table 1. Inert Ordnance Targets at Aberdeen Test Site**

<b>Standard Type</b>	<b>Nonstandard (NS)</b>
20-mm Projectile M55	20-mm Projectile M55
	20-mm Projectile M97
40-mm Grenade M385	40-mm Grenade M385
40-mm Projectile MkII Body	40-mm Projectile M813
BDU-28 Submunition	
BLU-26 Submunition	
M42 Submunition	
57-mm Projectile APC M86	
60-mm Mortar M49A3	60-mm Mortar (JPG)
	60-mm Mortar M49
2.75-inch Rocket M230	2.75-inch Rocket M230
	2.75-inch Rocket XM229
MK 118 Rockeye	
81-mm Mortar M374	81-mm Mortar (JPG)
	81-mm Mortar M374
105-mm HEAT Round M456	
105-mm Projectile M60	105-mm Projectile M60
155-mm Projectile M483A1	155-mm Projectile M483A
	500-lb Bomb

The purpose of the demonstration at a Standardized UXO Technology Demonstration Site is to evaluate the detection and discrimination capabilities of the technology being demonstrated. The evaluation objectives are: (a) Detection and discrimination under scenarios that vary targets and clutter, (b) Cost, time and manpower requirements. (c) Ability to analyze survey data in a timely manner and provide prioritized “Target Lists” with associated confidence levels, and (d) Collection of high quality, ground-truth, geo-referenced data for post-demonstration analysis.

The scoring of performance is conducted in two stages. These two stages are termed the response stage and the discrimination stage. For both stages, the probability of detection ( $P_D$ ) and the false

alarms are reported as receiver operating characteristic (ROC) curves. False alarms are divided into those anomalies that correspond to emplaced clutter items, measuring the probability of false positive ( $P_{FP}$ ), and those that do not correspond to any known item, termed background alarms.

The response stage scoring evaluates the ability of the system to detect emplaced targets without regard to ability to discriminate ordnance from other anomalies. For the blind grid response stage, the demonstrator provides the scoring committee with a target response from each and every grid square along with a noise level below which target responses are deemed insufficient to warrant further investigation. This list is generated with minimal processing and, since a value is provided for every grid square, will include signals both above and below the system noise level.

The discrimination stage evaluates the demonstrator's ability to correctly identify ordnance as such and to reject clutter. For the blind grid discrimination stage used here, the demonstrator provides the scoring committee with the output of the algorithms applied in the discrimination-stage processing for each grid square. The values in this list are prioritized based on the demonstrator's determination that a grid square is likely to contain ordnance. Thus, higher output values are indicative of higher confidence that an ordnance item is present at the specified location. For digital signal processing, priority ranking is based on algorithm output. For other discrimination approaches, priority ranking is based on human (subjective) judgment. The demonstrator also specifies the threshold in the prioritized ranking that provides optimum performance, (i.e. that is expected to retain all detected ordnance and rejects the maximum amount of clutter).

The demonstrator is also scored on efficiency and rejection ratio, which measures the effectiveness of the discrimination stage processing. The goal of discrimination is to retain the greatest number of ordnance detections from the anomaly list, while rejecting the maximum number of anomalies arising from non-ordnance items. Efficiency measures the fraction of detected ordnance retained after discrimination, while the rejection ratio measures the fraction of false alarms rejected. Both measures are defined relative to performance at the demonstrator-supplied level below which all responses are considered noise, i.e., the maximum ordnance detectable by the sensor and its accompanying false positive rate or background alarm rate.

### **1.3. Regulatory Drivers**

The regulatory issues affecting the UXO problem are most frequently associated with the BRAC and FUDS processes involving the transfer of DoD property to other agencies or to the civilian sector. When transfer of responsibility to other government agencies or to the civilian sector takes place, the DoD lands fall under the compliance requirements of the Superfund statutes. Section 2908 of the 1993 Public Law 103-160 requires adherence to CERCLA provisions. The basic issues center upon the assumption of liability for ordnance contamination on the previously DoD-controlled sites.

Historically, UXO clearance has relied on “mag and flag” (hand survey) operations in preparation for remediation. Such approaches are notoriously inefficient; many sources believe that much more than 50% of buried ordnance remains undetected and unrecovered using this approach [4]. Furthermore, “mag and flag” produces an uncertifiable survey product, unsuitable for quality control (QC) and quality assurance (QA) evaluations. Such operations leave no permanent record of actions taken for historical archives, and thus provide no documentable support or evidence in the event of litigation.

There are dozens of DoD facilities encompassing hundreds of thousands of acres of UXO-contaminated lands. An increasing fraction of these sites will be facing similar issues over the next decade. Additionally, active DoD ranges must be cleared periodically to allow for continued operations or for changes in facility use. Although different requirements apply in these situations, no automated or vehicular-based technologies are currently available to support military EOD teams in range clearance operations. Technologies exist to effectively remediate UXO and explosives waste contamination, but do not exist that can (1) effectively detect and discriminate between intact UXO and other ferrous materials; and (2) certify “cleared” lands as clean.

Electromagnetic induction is a technology appropriate for addressing the problem of discriminating between UXO and clutter. This demonstration will provide data that can be used to demonstrate a statistical probability of success for discrimination using a commercially available UXO sensor (Geonics EM61-HH).

#### **1.4. Stakeholder/End-User Issues**

There are no specific stakeholder/end-user issues.

## **2. Technology Description**

### **2.1. Technology Development and Application**

The Geonics EM61-HH handheld metal detector is a time domain or pulsed electro-magnetic induction (EMI) sensor (Figure 1). The transmitted primary field induces eddy currents in the target, which in turn radiate a secondary field measured by the receive coil. The EM61-HH measures the secondary field at time delays of 147  $\mu$ sec, 263  $\mu$ sec, 414  $\mu$ sec and 613  $\mu$ sec after the primary field shutoff. As a practical matter, the range of decay times measured by the EM61-HH is too early and too restricted to be of much use for target classification and discrimination. The restricted moment available from a handheld system makes it inevitable that late-time (> a few msec) returns from most UXO will not be above the noise.

Handheld sensor weight and power limitations adversely affect on detection and discrimination performance in other ways. This is quite obvious from the demonstration results discussed in sections 2.4 and 4.2 below – the sensor transmit moment is simply too small to allow detection and discrimination of typical UXO targets at depths greater than a few tens of centimeters.



**Figure 1. Electromagnetic induction and the EM61-HH sensor head.**

For targets that are within the sensor's useful range, the response varies in a predictable way with target size, shape and orientation, which can be exploited for target classification. Our discrimination approach [1] uses a model-based estimation procedure to determine whether or not an unknown target is likely to be a UXO item. It entails estimating the size and shape of the target from the spatial pattern of the induced field above the target. The EM61 signal is a linear function of the flux through the receiving coil. In our model, the flux is assumed to originate from an induced dipole moment at the target location given by

$$\mathbf{m} = \mathbf{UBU}^T \mathbf{H}_0$$

where  $\mathbf{H}_0$  is the peak primary field at the target,  $\mathbf{U}$  is the transformation matrix between the coordinate directions and the principal axes of the target, and  $\mathbf{B}$  is an empirically determined, effective magnetic polarizability matrix. For an arbitrary compact object, this matrix can be diagonalized about three primary body axes and written as:

$$\mathbf{B} = \begin{bmatrix} \beta_X & 0 & 0 \\ 0 & \beta_Y & 0 \\ 0 & 0 & \beta_Z \end{bmatrix}.$$

The relative magnitudes of the  $\beta$ 's are determined by the size, shape and composition of the object as well as the transmit pulse waveform and the delay time after the primary field shutoff at

which the secondary field is measured. The transformation matrix contains the angular information about the orientation of these body axes.

For cylindrical objects like most UXO, B is a diagonal matrix with only two unique coefficients, corresponding to the longitudinal ( $\beta_L$ ) and transverse ( $\beta_T$ ) directions:

$$B = \begin{bmatrix} \beta_L & 0 & 0 \\ 0 & \beta_T & 0 \\ 0 & 0 & \beta_T \end{bmatrix}.$$

Discrimination is based on target  $\beta$ 's estimated from spatially mapped data. Specific ordnance items have specific  $\beta$  values, while clutter items generally have three distinct  $\beta$  values.

The standard EM61-HH (Figure 2, left hand picture) consists of a sensor head mounted on a shaft, a backpack containing battery power and electronics, and a PRO 4000 field handheld field computer for data acquisition. The equipment has been assembled in a cart for use in cued identification as shown in the center and right pictures in Figure 2.



**Figure 2. Geonics EM61-HH (left) and setup for cued identification (center, right).**

Since this is a cued identification system, target locations are known and have been flagged. Data are collected above each target on a 75 cm square, 6x6 point grid with the EM61-HH. A plywood grid template is first placed on the ground over the target (Figure 3). Grid points are marked on the template at the intersections of two perpendicular sets of lines. The line spacing is 15 cm and there are six lines in each set. A piece of Plexiglas marked with crosshairs is attached to the bottom of the sensor head. The EM61-HH sensor head is placed flat on the plywood template. It is precisely aligned and located at the grid points by lining up the crosshairs on the sensor head with the grid lines on the template. The positioning error is believed to be on the order of a few mm. Our experience with test stand data and data collected at a seeded site is that the grid does not need to be precisely centered over the target. Actual target location relative to the center of the grid is determined as part of the data inversion. Sensor readings are averaged for

a couple of seconds at each grid point, and leveled using blank readings taken off to the side of the template. The data collection takes about 5 minutes per target. This simply reflects the time required to align the sensor and collect a couple of seconds of data at each grid point, as well as recording background levels before and after the grid. The event marker is used to identify background data readings and readings at the grid points.



**Figure 3. EM61-HH grid template.**

EM61-HH data are recorded using the handheld field computer that is part of the standard equipment package. The data are downloaded via serial port to a notebook computer for processing. Processing and analysis on the notebook is done using a set of IDL routines that extract the background and grid point readings identified by event marks, allow display and editing of the data, calculation of the target location, depth and polarizability eigenvalues, and determination of target size and likelihood that it is ordnance or clutter. The procedures for target fitting run significantly faster than the time required to collect the data.

As noted previously, the EM61-HH measures the secondary field at time delays of 147  $\mu\text{sec}$ , 263  $\mu\text{sec}$ , 414  $\mu\text{sec}$  and 613  $\mu\text{sec}$  after the primary field shutoff. Over this time range, the response for UXO and other steel objects of comparable size decays algebraically. Eventually, after the eddy currents diffuse through target the EMI response rolls off exponentially. The rate depends on shape, material, and thickness (diffusion time  $<1$  msec for sheet metal of thickness  $<2$  mm). It turns out that the ratio of the response in the last gate to that in the first gate can be used for identifying thin sheet metal, wire scrap, etc. (see Figure 4). The plot shows the ratio of average EM61-HH signals at 613  $\mu\text{sec}$  and 147  $\mu\text{sec}$  for sheet metal scrap items. The ratio for UXO is 0.14 to 0.25 based on over 70 measurements of ordnance items ranging in size from 20mm projectiles to 8" rounds.

As a practical matter, this aspect of the EM61-HH did not figure significantly in the demonstration. A color-coded display of the ratio is included in the processing interface (see

Figure 13). However, few, if any of the targets at the Aberdeen Blind Test Grid showed up as clearly non-ordnance because of a very low gate ratio. Consequently, for this demonstration the spatial (grid) data ends up being the primary input to target classification and discrimination, and for the most part, we only use the first time gate for discrimination.

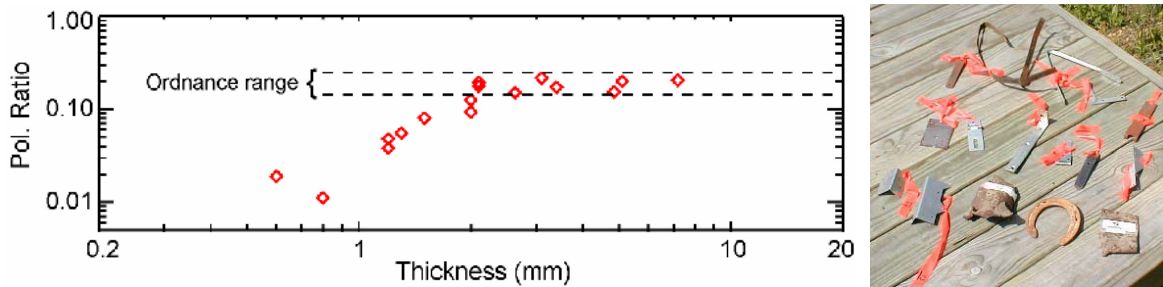


**Figure 4. Ratio of EM61-HH signal at last time gate to signal at first time gate for thin walled scrap metal compared to UXO.**

The grid data are inverted to determine target features or attributes that are used for target classification and discrimination. The inversion is implemented by performing a least-squares fit of the data to a dipole response model. The model parameters are target X, Y location relative to the grid, target depth, eigenvalues of the polarizability tensor ( $\beta$ 's) and target orientation. Target classification is based on comparing the  $\beta$ 's from the grid data to library values determined from controlled measurements of the expected UXO types (see section 2.2 below). In some situations (depending on target size, orientation and distance from the sensor head) there is a bit of ambiguity regarding the "correct" values of the  $\beta$ 's and the depth. We suspect that this is due to failure of the dipole response model to faithfully reproduce the signal when there dimensions of the target are comparable to distances over which there are significant changes in the primary field (and the reciprocal received field). For most UXO, there is one large  $\beta$  corresponding to the axial response and two smaller, equal  $\beta$ 's corresponding to transverse responses. With ordnance items on a test stand, we find that the depth at which the secondary  $\beta$ 's are equal is not always the depth that minimizes the RMS deviation between the data and the dipole model. Consequently, we find it best to actually sweep through depth looking at the best fit eigenvalues and residual error as functions of depth.

This is illustrated in Figures 5, where we "focus" a grid over the 2.75 inch rocket warhead as a function of depth. The plots show the trajectory of the solution (fit error and betas vs. assumed target depth) with the rocket in different orientations, nominally 40cm below the sensor. On the left, the rocket is flat. The upper plot is the RMS error between the grid data and the dipole model fit as a function of the assumed target depth. The lower plot shows the corresponding betas. Color encodes error relative to the minimum: in the green region it is close to the minimum. Red starts when the error is more than three times the minimum. The focal depth at which the inversion matches a cylindrical target (equal secondary betas) is about 5 cm above the

depth at which the RMS deviation between the data and the dipole model fit is minimized. Even though this point is not the minimum error fit, it is still good, with an RMS error equal to 1% of the peak signal. The corresponding plots in the center and right are for the rocket in 45° nose down and vertical nose down orientations, respectively. The beta values for all three grids are essentially the same at the focal depths indicated by the dotted vertical lines.

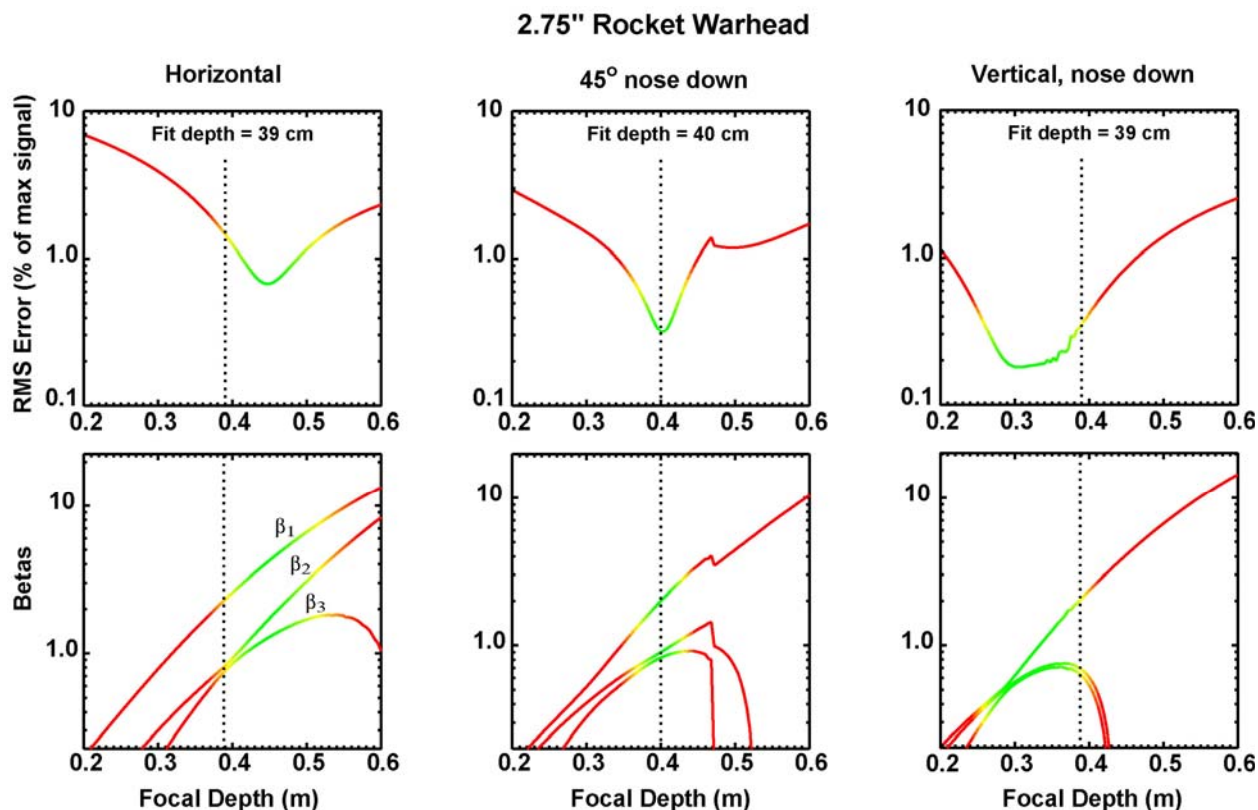


**Figure 5. Fit error (top) and beta (bottom) trajectories vs. focal depth for inversion of grid data over 2.75 inch rocket warhead in different orientations.**

We built up a library of UXO  $\beta$ 's from test stand measurements on the standard UXO items from the Aberdeen Test Center. Typically, we collected six grids over each item, with the object at six different orientations. The “correct” set of  $\beta$ s for each item was chosen as the median of the results for the different orientations, subject to the constraint that the secondary  $\beta$ s were degenerate (equal). We find that with a few exceptions (notably the larger items oriented vertically) all of the sets of  $\beta$ s for each object are within 25% of a nominal or “correct” value. That is, they live in a “beta cloud” that has a radius of about 25% of the center value.

## 2.2. Previous Testing of the Technology

Bench testing occurred during the summer of 2002 at a site outside Buckeystown, Maryland. The purpose of this testing was to acquire a response library for the standard ordnance items emplaced at the Aberdeen Standardized Test Site. We also measured the response of a set of representative clutter items from the Aberdeen Test Center. The standard ordnance items and clutter objects are shown in Figure 6.



**Figure 6. Standard inert ordnance items (left) and clutter from ATC (right).**

Data were collected on the nonmetallic test stand shown in Figure 7. Test stand data collection included 95 grids over the 14 ordnance items at different depths and orientations (data for the largest items were collected over the ATC test pit) and 50 grids over the 15 clutter items. Typically, we collected six grids over each ordnance item, with the object at six different orientations. Most clutter items were measured at three different orientations.



**Figure 7. Nonmetallic test stand for controlled testing the EM61-HH system.**

First time gate (147 msec) polarizability eigenvalues determined by inverting the grid data for the targets are shown in the various plots in Figure 8. The  $\beta$ s are plotted as a vertical line from the smallest to the middle  $\beta$ , located at an abscissa (horizontal axis) value equal to the largest  $\beta$ . For the smaller targets (submunitions and 20mm projectile),  $\beta$ s for the different grids form a tight cloud. The beta clouds spread out for the larger projectiles and the mortars. Large projectiles in vertical, nose up position are conspicuous outliers.

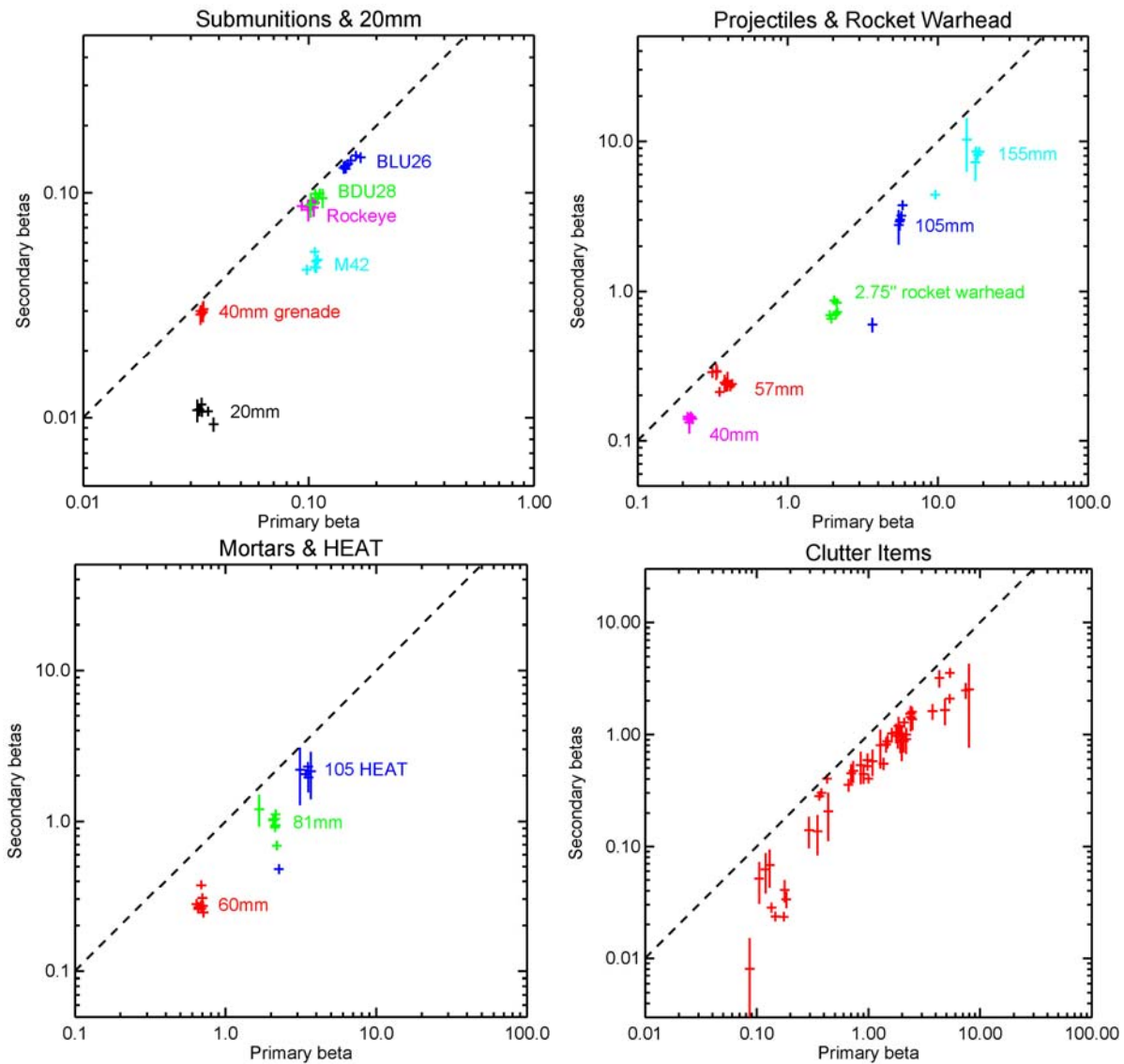


**Figure 8.  $\beta$ s for ordnance and clutter determined from test stand measurements.**

A preliminary estimate of discrimination potential was made using the test stand data, including test stand measurements of a 76mm projectile, but not including the test pit measurements of the 105mm, 105 HEAT and 155mm projectiles. We found that 79 of 83 ordnance signatures had their  $\beta$ s within 25% of the nominal value for that item. That is, they lived in a "beta cloud" that has a radius of about 25% of the center value. The outliers were: 76mm nose up, 60mm nose up, 81mm nose down and 81mm 45° down. When compared with the library ordnance  $\beta$ 's, 13 out of the 50 clutter measurements fell within one of the UXOs 25% beta clouds. Using the 25% beta radius as a threshold, the expected probability of detection ( $P_D$ ) is then 95%, while the expected probability of False Positive ( $P_{FP}$ ) is 26%. The false alarm rate increases to 20 out of 50 (40%) when the threshold beta radius is increased enough to capture all the ordnance signatures.

### **2.3. Factors Affecting Cost and Performance**

The primary cost factor is manpower for data collection. Data collection generally takes significantly longer than data processing. The Blind Grid data collection proceeded very quickly and efficiently. This was because the targets were spaced out every two meters along a regular pattern of lanes. During the demonstration, it took an average of 16.77 minutes to traverse a lane checking each cell for an above-threshold (~40 mV) response, and an average of 2.86 minutes to collect data over each cell that gave an above-threshold response. It took two days to interrogate all 400 grid cells. The system has subsequently been used by a commercial team on a UXO cleanup site in New England [5]. There, the targets were anomalies picked from a standard EM61 survey and had to be re-acquired before the EM61-HH grid data could be collected. The production rate at that site was about 30 targets per day.

Good performance requires a well motivated operator who is careful to align the sensor properly and collect a few seconds of data at each grid point. Accurate inversion requires highly accurate positioning. We found that the commercial team from NAEVA Geophysics was capable of collecting good data that could support inversion. Give good data, the major problem with all of the discrimination schemes in use today is that they rely on a priori knowledge of the possible UXO targets and their EMI signatures. A target is declared non-ordnance if its "features" (betas for the EM61-HH) do not match up with those of one of the possible UXO targets. If, as in the Standardized UXO Demonstration Sites, there are a relatively large number of possible UXO targets, the region of feature space occupied by possible UXO targets is relatively large, and it is likely that much of the clutter will be misclassified as ordnance. Missed detections can occur when there are anomalous signatures (e.g. large UXOs oriented vertically) or when UXO targets are not included in the signature or feature library (e.g. nonstandard targets).

### **2.4. Advantages and Limitations of the Technology**

The EM61-HH is a standard commercial UXO sensor. It is quite portable, and well suited to the task of cued identification. Because of the size of the coils and the transmitted power, it is more effective for the smaller, more shallow targets than the larger, deeper targets. Handheld total

field magnetometer systems (e.g. Geometrics G858) may be more effective in detecting large, deep targets, but have limited target classification ability. Other handheld EMI systems (e.g. White's, Minelab, Geophex) have detection envelopes similar to the EM61-HH. Of these, only the Geophex GEM-3 broadband EMI sensor (Figure 9) has been demonstrated at the Aberdeen Standardized UXO Demonstration Site [6].



**Figure 9. GEM-3 handheld broadband EMI sensor.**

We can compare the performances of the EM61-HH and the GEM-3 (handheld mode) using the standard performance criteria *Efficiency* and *False Positive Rejection Rate* (see section 4). Efficiency measures the degree to which the detection performance of the sensor system is preserved after application of discrimination techniques. Efficiency is a number between 0 and 1. An Efficiency of 1 implies that all of the ordnance items initially detected in the Response Stage were retained at the discrimination stage. The Efficiency of the EM61-HH was 0.83, while that of the GEM-3 was 0.76. The False Positive Rejection Rate measures the degree to which the sensor system's false positive performance is improved over the Response Stage false positive performance. The Rejection Rate is a number between 0 and 1. A Rejection Rate of 1 implies that all emplaced clutter items initially detected in the Response Stage were correctly rejected at the Discrimination Stage. The Rejection Rate for the EM61-HH was 0.49, while that of the GEM-3 was 0.40. The EM61-HH performed somewhat better than the GEM-3 by both measures. Performance for Blind Grid demonstrations that have been scored to date [6-14] is summarized in Table 2. Also included in Table 2 are the Response Stage Probability of Detection (Pd) and Probability of False Positive (Pfp), which form the basis on which Efficiency and Rejection Ratio are calculated. Note that there have been several demonstrations using the GEM-3 in various configurations (handheld, cart mounted, towed array).

**Table 2. ATC Blind Grid Demonstration Performance Summary**

<b>Demonstrator</b>	<b>Scoring Report</b>	<b>Pd</b>	<b>Pfp</b>	<b>Efficiency</b>	<b>Rejection Ratio</b>
<i>Zonge 4D-TEM</i>	37	0.80	0.90	0.55	0.55
<i>AETC EM61-HH</i>	39	0.65	0.65	0.83	0.49
<i>Witten 200MHz Cart</i>	45	0.70	0.75	0.85	0.21
<i>Geophex GEM 3 Pushcart</i>	49	0.85	0.85	0.82	0.19
<i>Geophex GEM 3 Handheld</i>	50	0.80	0.85	0.76	0.40
<i>Geophex GEM 3 Towed Array</i>	125	0.30	0.40	0.71	0.22
<i>NRL MTADS GEM Towed Array</i>	127	0.85	0.95	0.92	0.30
<i>ERDC GEM 3 Pushcart (Standard)</i>	141	0.25	0.30	1.00	0.00
<i>ERDC GEM 3 Pushcart (Enhanced)</i>	142	0.60	0.65	1.00	0.00

### **3. Demonstration Design**

#### **3.1. Performance Objectives**

The primary quantitative performance criteria are Detection Efficiency and False Alarm Rejection Rate. Efficiency measures the degree to which the detection performance of the sensor system is preserved after application of discrimination techniques. Efficiency is a number between 0 and 1. An efficiency of 1 implies that all of the ordnance items initially detected in the response stage were retained at the discrimination stage. The False Positive Rejection Rate measures the degree to which the sensor system's false positive performance is improved over the response stage false positive performance. The rejection rate is a number between 0 and 1. A rejection rate of 1 implies that all emplaced clutter items initially detected in the response stage were correctly rejected at the discrimination stage.

#### **3.2. Selecting Test Sites**

The demonstration was carried out on the Blind Grid at the Standardized UXO Technology Demonstration Site at the Aberdeen Test Center. This site was selected in consultation with the ESTCP Program Manager. Testing at this site is independently administered and analyzed by the government for the purposes of characterizing technologies, tracking performance with system development, comparing performance of different systems, and comparing performance in different environments.

### 3.3. Test Site History/Characteristics

The Standardized UXO Technology Demonstration Site Program is a multi-agency program spearheaded by the U.S. Army Environmental Center. The U.S. Army Aberdeen Test Center (ATC) and the U.S. Army Edgewood Research, Development and Engineering Center provide programmatic support. The program is being funded and supported by ESTCP, SERDP and the Army Environmental Quality Technology Program. Figure 10 shows an overview of the Standardized UXO Technology Demonstration Site at Aberdeen and the location of the Blind Test Grid.

The Calibration Lanes are adjacent to the Blind Test Grid. Calibration lanes are designed to provide the demonstrator with a sensor library of standardized and calibration targets prior of entering the test field. Two lanes contain varying size copper wire hoops. One of those lanes also contains four steel spheres. Another lane has ¼ inch steel flat plates designed to test radar systems. The rest of the lanes are made up of ordnance items. Figure 11 shows the layout of the Calibration Lanes. The ordnance types in the Calibration Lanes are as indicated in the figure. Some of the data collected at the calibration site were used with the test stand data to assemble the library of polarizability coefficients for the ordnance targets.



**Figure 10. UXO Technology Demonstration Site at Aberdeen Test Center.**

The Standardized UXO Technology Demonstration Site Review Committee developed the following parameters for the layout of the Calibration Lanes:

- (1) Munitions that are generally elongated in shape (aspect ratio not equal to one) are placed into the ground in six orientations and at three different depths.
- (2) Munitions generally round in shape (aspect ratio of one) are buried at three different depths.
- (3) The first and last opportunity of each calibration lane contains a 3.6-kg steel ball buried at 15 cm to provide a uniform signature that can be easily identified when looking at the raw data.
- (4) The spacing between munitions under 89 mm in diameter is 2 meters center-to-center.

- (5) The spacing between munitions greater than 89 mm in diameter is 3 meters center-to-center.
- (6) Between each calibration lane for munitions smaller than 89 mm is a 1-meter wide travel lane.
- (7) For munitions greater than 89 mm, a one-meter wide extra travel lane is added to increase the distance between munitions and reduce signature overlap.
- (8) One lane has four 5.4-kg steel sphere (shot put) buried between 0.5 to 2 meters in 0.5 meter increments to test the sensor's maximum depth detection capabilities.
- (9) Another lane has 12-, 16-, 18- and 20-gauge uncoated copper wire hoops (15- and 30-cm diameter) buried at 0.3 meter.
- (10) A third lane has two each 1 cm thick by 30- and 61-cm diameter circular steel plates buried at 30 and 91 cm.

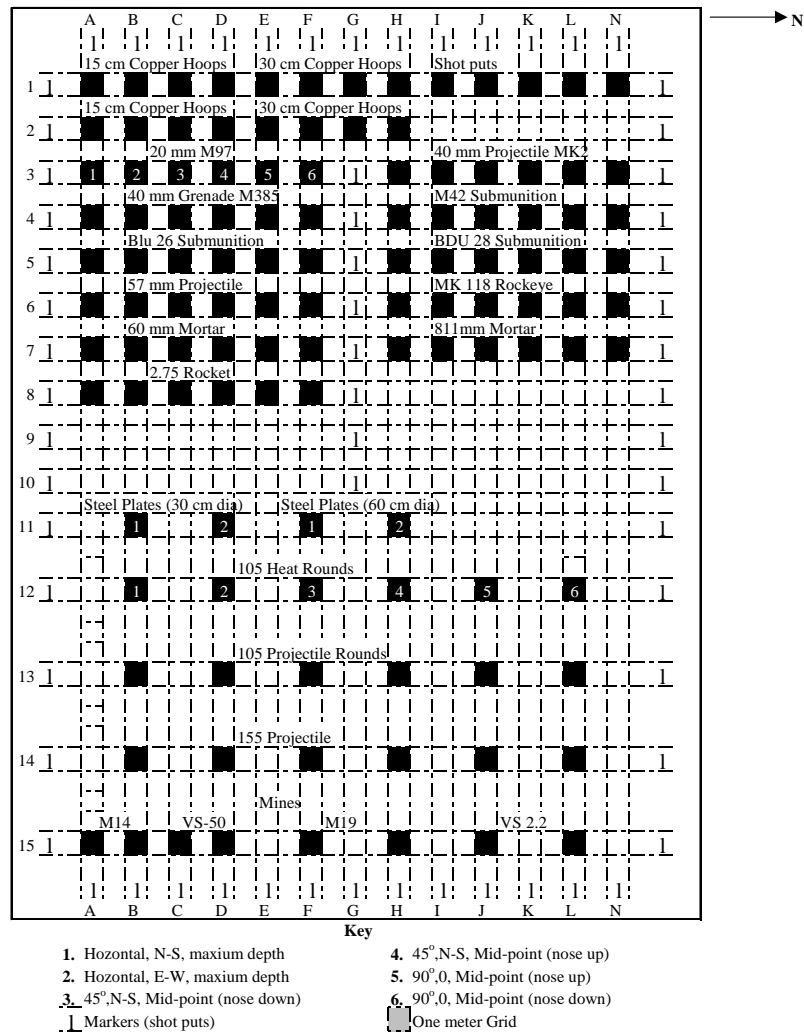


**Figure 11. Layout of Calibration Lanes.**

The Blind Test Grid is designed to test a demonstrator's ability to detect and discriminate clutter from ordnance under controlled parameters. These controlled parameters are designed to reduce the vibration noise when moving the equipment by smoothing out the field. Referencing an emplaced grid system also eliminates navigational errors. The grid system is clearly marked so demonstrators will know their location on the field at all times. At the center of each cell within the grid there are three target possibilities - nothing, clutter, or ordnance. The Blind Test Grid has 400 opportunities. Figure 12 is an example layout of the Blind Test Grid.

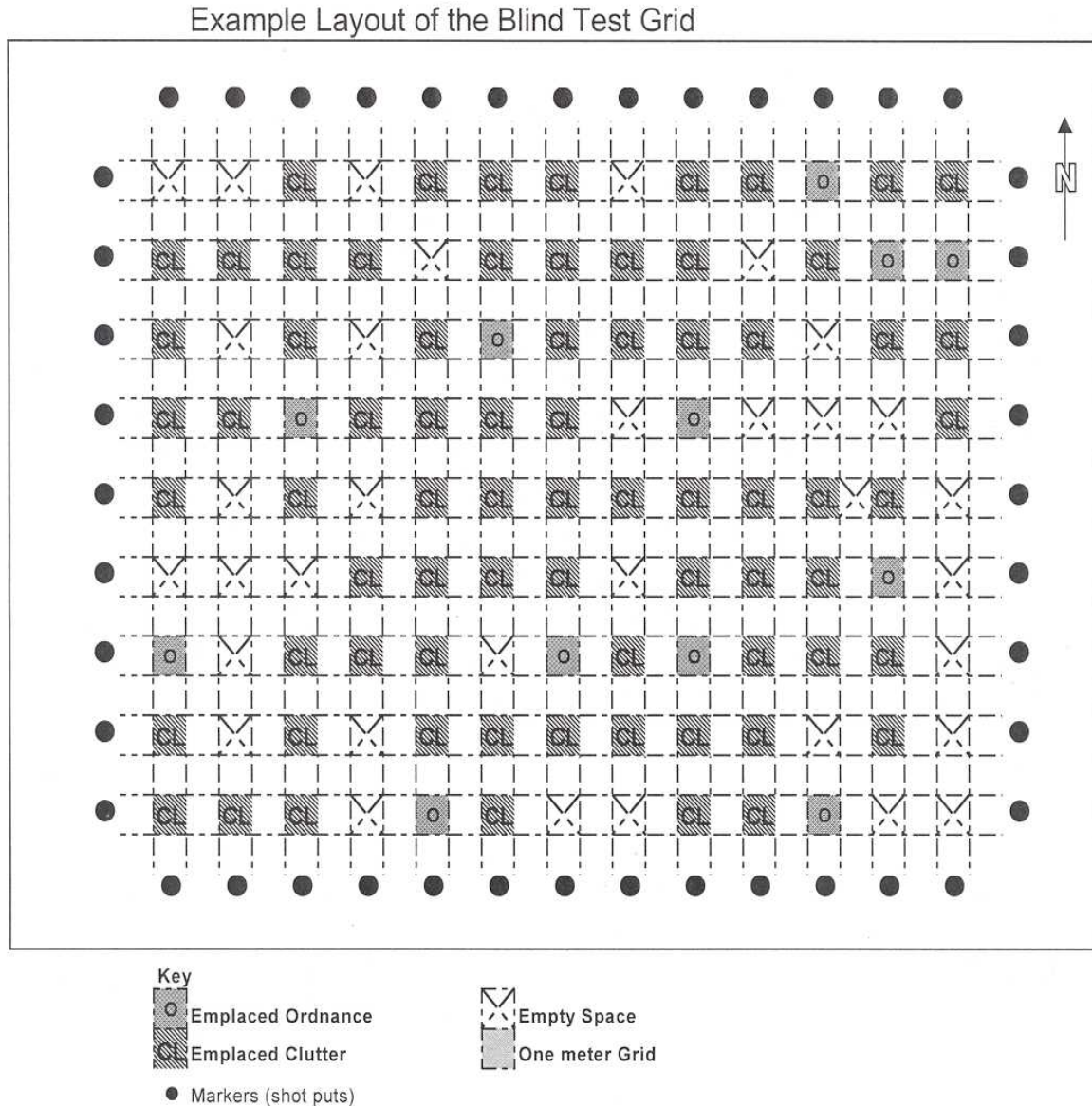


**Figure 12. Layout of Blind Test Grid.**

### **3.4. Present Operations**

Subsequent to the demonstration, the technology has been used to support a UXO cleanup action at a site in Bridgeport, Connecticut [5].

### **3.5. Pre-Demonstration Testing and Analysis**

Pre-demonstration testing is described in section 2.2 above.

### **3.6. Testing and Evaluation Plan**

#### **3.6.1. Demonstration Set-Up and Start-Up**

Demonstration set-up and start-up consisted of connecting instrument and battery cables and flagging nominal target locations in the Calibration Lanes and the Blind Grid. The corners of the target grid cells in the Calibration Lanes and the Blind Grid are marked with PVC pipes flush with the ground. We placed a plastic stake flag in the center of each grid cell. Each flag was marked with the appropriate grid cell number, e.g. "H14".

#### **3.6.2. Period of Operation**

**Table 3. Period of Operation of the Demonstration at ATC**

<b>Demonstration Phase</b>	<b>Period of Operation</b>
Survey Calibration Lanes	October 21, 2002
Survey Blind Grid	October 22-23, 2002

#### **3.6.3. Area Characterized**

The Calibration Lanes and the Blind Grid were characterized. The area of the Calibration Lanes is 25x35 m. The area of the Blind Grid is 40x40 m.

#### **3.6.4. Residuals Handling**

This demonstration did not produce any residuals.

#### **3.6.5. Operating Parameters for the Technology**

The EM61-HH was operated in the standard survey mode at a data rate of ten readings per second.

### 3.6.6. Experimental Design

Data were collected lane by lane. In the Blind Grid, there are twenty lanes (numbered A through T). Each lane has twenty grid cells (numbered 1 through 20). In each grid cell there may be one or more UXO or clutter items, or nothing. Stake flags numbered by lane and cell (e.g. H07) were placed in the center of each grid cell during set-up (section 3.6.1). Data for each lane were recorded in a separate data file identified by year, Julian date, and sequential file number, e.g. file 02296007 for the seventh (007) file collected on October 23rd, 2002 (year 02, day 296).

We would create a new file in the data logger at the start of each lane, then proceed down the lane, stopping at each grid cell. The status of each grid cell (weak or no response, or survey line number for recorded data) was entered in a log book. The EM61-HH was running continuously, but data logging was limited to grid cells where there was a response over the center of the cell that was large enough to support inversion. The sensor was waved around over the center of the cell while the sensor reading was monitored on the data recorder. If the response was deemed large enough (usually greater than ~40 mv), then the grid template was placed over the cell, a new “survey line” was started in the data recorder, and data were recorded at each of the template grid points. Blank readings to the side of the grid cell were also recorded before and after the template readings. Data were recorded continuously. The event marker (button) was used to mark data segments corresponding to blanks and data points at the template grid points. A few seconds of data were recorded at each template grid point. During production, visiting target cells spaced two meters apart, the routine nature of the data collection resulted in a faster rate of data collection than the nominal five minutes per target that we would expect in the field. It took an average of 16.77 minutes to traverse a lane checking each cell for an above-threshold response, and an average of 2.86 minutes to collect data over each cell that gave an above-threshold response.

Data were processed using a set of IDL procedures. First, the data were downloaded from the data recorder to a PC and unpacked to ASCII files using the standard Geonics EM61 software that comes with the instrument. The each data file was split into grids. Each 6x6 point data grid was labeled by the corresponding lane and cell number in the Blind Grid. The data for each 6x6 point data grid were leveled using the before and after blanks, and the readings at each point were averaged. The spatially mapped data were then inverted. Figure 13 shows the processing interface. It contains six plots that show all of the relevant fit information for the target. The two on the left show comparisons between the model fit and the data. The upper left figure is a scatter plot of model vs. data at the fit depth. (The grid cell identifier has been replaced by XXX to protect the integrity of the Blind Grid.) The points should follow the diagonal. The lower left figure shows a contour plot of the array data with the model fit contoured with dashed lines. Note that the area covered by the data array is 75 cm by 75 cm. The contour maps are superimposed on a colorized map of the ratio of the last time gate signal to the first time gate signal. We have observed that aluminum and other non-ferrous targets often have a large value for this ratio, and show up as deep red. Thin-walled steel targets (i.e., sheet metal or wire less than about 1.5 mm thick) usually have a low ratio, and show us as deep blue. Ordnance and other steel items have

variable color maps. This target fits quite well to a 60mm mortar, and as expected has a gate ratio that ranges between 0.1 and 0.2. The upper middle figure is a plot of RMS error in the model fit vs. the focus depth. It shows how well the array can be focused as a function of depth. The color coding visually indicates the focus quality: green is good, red is bad. The upper right figure shows apparent target inclination and azimuth as functions of focus depth, again color-coded. This target appears to be flat (inclination  $0^\circ$ ) and at an azimuth angle of  $60^\circ$ . The lower middle and right figures show the first time gate  $\beta$ s and how they vary as the focus depth is changed. The lower middle shows the three betas as functions of depth. The lower right is the most useful figure. It is a plot of the two smaller betas as a function of the largest beta as we sweep over focus depth. The horizontal axis is for the largest beta. Symbols are the averages of the two smaller betas, and the vertical lines run from one to the other of the smaller betas. The black circle shows the expected beta-range for a 60mm mortar determined from the test stand data.

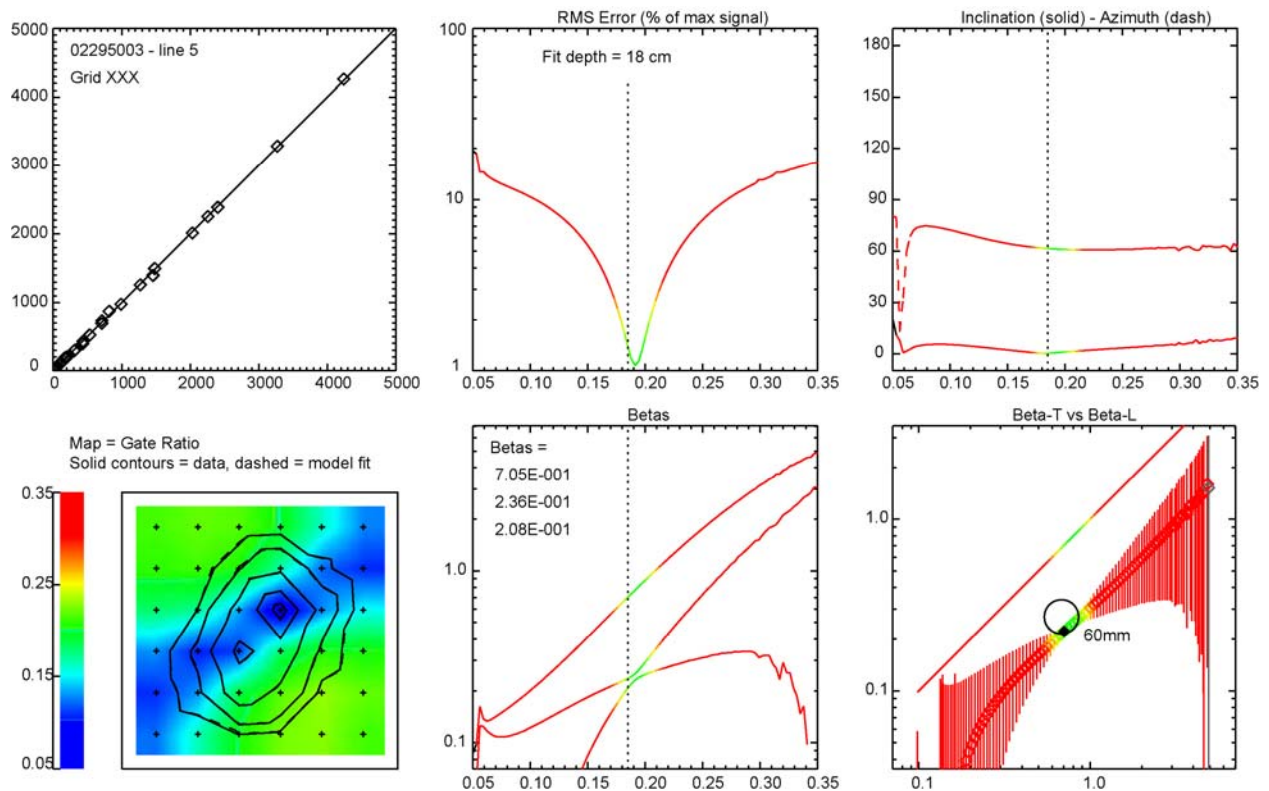


**Figure 13. User interface for inversion and target classification (see text).**

Inversion results for each cell were compared with  $\beta$ s for all of the 14 possible ordnance items. A target was declared ordnance (and named) if its  $\beta$ s matched up with one of the possible ordnance targets to within the 25% beta circle. We also checked for possible outliers by comparing with beta trajectories for the larger ordnance items in vertical orientation. On the basis of the inversion all of the interrogated targets were assigned a ranking between 1 and 6. A ranking of 1 (high

confidence ordnance) was used for targets that gave essentially perfect matches to one of the ordnance beta sets. A ranking of 6 (high confidence clutter) was given to targets that could not possibly be matched up any of the expected ordnance targets. Rankings of 3 and 4 were used for targets where the fit quality was poor and it was difficult to tell precisely how well the possible ordnance targets could reproduce the data. Within each category (1-6), the targets were sorted in order of increasing “beta distance” to the best fitting ordnance target. The best fitting ordnance target is the one whose betas ( $\beta_L$  and  $\beta_T$  determined from the test stand data as described in section 2.2) come closest to the inversion trajectory as in the lower right graph in Figure 13. If  $(\beta_1, \beta_2, \beta_3)$  are the inversion  $\beta$ s at the point of closest approach to  $(\beta_L, \beta_T, \beta_T)$ , then the beta distance is defined as

$$\beta_{\text{dist}} = \frac{\sqrt{(\beta_1 - \beta_L)^2 + (\beta_2 - \beta_T)^2 + (\beta_3 - \beta_T)^2}}{\sqrt{\beta_L^2 + 2\beta_T^2}}.$$

The discrimination stage response was the net resultant rank ordering of the targets. A discrimination stage response of 1 was assigned to the category 6 (high confidence clutter) target with the largest beta distance. A discrimination stage response of 2 was assigned to the category 6 (high confidence clutter) target with the second largest beta distance. The highest discrimination stage response was assigned to the category 1 (high confidence ordnance) target with the smallest beta distance. Targets that had below threshold responses (and therefore were not interrogated using the EM61-HH grid) were more or less arbitrarily assigned discrimination stage responses between 0 and 1 to permit generation of a smooth ROC curve.

### 3.6.7. Sampling Plan

The demonstration did not involve an explicit sampling plan. All Blind Grid cells were visited in order, lane by lane. Only those grid cells with a response above the threshold for discrimination (~40 mv) were interrogated using the EM61-HH on the grid template.

### 3.6.8. Demobilization

Demobilization consisted of pulling up the stake flags and packing the EM61-HH gear in the back of a car. Breakdown and packing of the gear takes about ½ hour.

## 4. Performance Assessment

### 4.1. Performance Criteria

Table 4 lists the performance criteria for the demonstration and the corresponding expected performance. Detection *Efficiency* measures the degree to which the detection performance of the sensor system is preserved after application of discrimination techniques. Efficiency is a

number between 0 and 1. An Efficiency of 1 implies that all of the ordnance items initially detected in the Response Stage were retained at the discrimination stage. The False Positive *Rejection Rate* measures the degree to which the sensor system's false positive performance is improved over the Response Stage false positive performance. The Rejection Rate is a number between 0 and 1. A Rejection Rate of 1 implies that all emplaced clutter items initially detected in the Response Stage were correctly rejected at the Discrimination Stage. Our *Expected* values for Efficiency and Rejection Rate are based on the test stand results described in section 2.2 above.

**Table 4. Performance Criteria for Demonstration**

<b>Type of Performance Objective</b>	<b>Primary Performance Criteria</b>	<b>Expected Performance (Metric)</b>
Qualitative	<i>1. Ease of Use</i>	Operator acceptance
Quantitative	<i>1. Detection Efficiency</i>	0.95
	<i>2. False Positive Rejection Rate</i>	0.74

#### 4.2. Performance Confirmation Methods

The quantitative performance objectives were evaluated under auspices of the Standardized UXO Technology Demonstration Site Program [9]. The expected and actual (as confirmed by the government evaluation) performance is summarized in Table 5.

**Table 5. Expected Performance and Performance Confirmation Methods**

<b>Performance Criteria</b>	<b>Expected</b>	<b>Confirmation Method</b>	<b>Actual</b>
Response Stage		Government Evaluation	
1. Probability of Detection	*		0.65
2. Probability of False Alarm	*		0.65
3. Background Alarms	*		0.10
Discrimination Stage		Government Evaluation	
1. Probability of Detection	*		0.55
2. Probability of False Alarm	*		0.30
3. Background Alarms	*		0.00
4. Efficiency	0.95		0.83
5. Rejection Rate	0.74		0.49

\* Unknown – depends on target size/depth distribution and clutter

It is not possible to assign values to the *Expected Performance* for Response Stage Probability of Detection, Probability of False Alarm, or Probability of Background Alarm. They depend on unknown, site specific parameters relating to the emplaced target size, depth and orientation distribution and the amount of residual clutter at the site which was not removed before the site became operational. The same holds true for these quantities at the Discrimination Stage since they are a dilution of the corresponding Response Stage quantities effected by the Discrimination Stage processing. The *Actual* values for Efficiency and Rejection Rate reported in Table 5 are based on a Discrimination Stage threshold level of 60mv.

The *Ease of Use* was a qualitative performance objective for the EM61-HH. We believe that it was met during the demonstration. This was confirmed by the operator and by the time required to collect the data on the Blind Grid. All 400 grid cells were interrogated during a two-day period. As noted previously, the system has subsequently been used by a commercial team on a live site [5]. There, the targets were anomalies picked from a standard EM61 survey and had to be re-acquired before the EM61-HH grid data could be collected. The production rate at that site was about 30 targets per day.

**Table 6. Complete Summary of Blind Grid Performance**

Metric	Overall	Standard	Nonstandard	By Size			By Depth, m		
				Small	Medium	Large	<0.3	0.3-1	> 1
<b>RESPONSE STAGE</b>									
Pd	0.65	0.65	0.65	0.85	0.50	0.40	1.00	0.40	0.00
Pd Low 90% Conf	0.58	0.56	0.51	0.74	0.36	0.19	0.95	0.27	0.00
Pfp	0.65	-	-	-	-	-	0.70	0.55	0.60
Pfp Low 90% Conf	0.56	-	-	-	-	-	0.60	0.44	0.25
Pba	0.10	-	-	-	-	-	-	-	-
<b>DISCRIMINATION STAGE</b>									
Pd	0.55	0.55	0.50	0.70	0.40	0.30	0.85	0.30	0.00
Pd Low 90% Conf	0.47	0.46	0.39	0.58	0.30	0.12	0.74	0.21	0.00
Pfp	0.30	-	-	-	-	-	0.30	0.35	0.40
Pfp Low 90% Conf	0.26	-	-	-	-	-	0.21	0.24	0.11
Pba	0.00	-	-	-	-	-	-	-	-

The complete summary of results provided by the Standardized UXO Technology Demonstration Site Scoring Committee [9] is reproduced in Table 6. The results are not unexpected. At the response stage, Pd and Pfp are both 65% - two thirds of the targets are detected by the EM61-HH. The breakdown by depth is telling. Shallow targets (<30 cm deep) are reliably detected, while targets below one meter cannot be detected. We believe that this trend reflects the characteristics of the sensor. The EM61-HH has relatively small coils and is best suited for detection and discrimination of shallow targets. In comparison, the NRL GEM array detected about 90% of the targets in the blind grid (see Table 2). At the discrimination stage, probability of misidentifying a clutter item as UXO (Pfp) hovers around 30%, compared to 26% for the test stand results. Probability of correctly identifying a UXO item as UXO (Pd)

decreases systematically from 85% for shallow (<30cm) targets to 0 for deep (>1m) targets, in roughly the same proportion as probability of detection at the response stage.

### 4.3. Data Analysis, Interpretation and Evaluation

The ROC curves for the EM61-HH are shown in Figure 14, which is a copy of Figure 2 in the EM61-HH Blind Grid Scoring Report [7]. The blue curve plots the Discrimination Stage Probability of Detection (correctly identifying ordnance as ordnance) as a function of Probability of False Positive (identifying clutter as ordnance). The dotted red curve gives the corresponding performance at the Response Stage. It represents the discrimination performance that would be realized if discrimination were based solely on signal strength (i.e., assuming that the strongest anomalies were ordnance and the weakest, clutter). Along the red curve, signal strength increases from the upper right to the lower left.

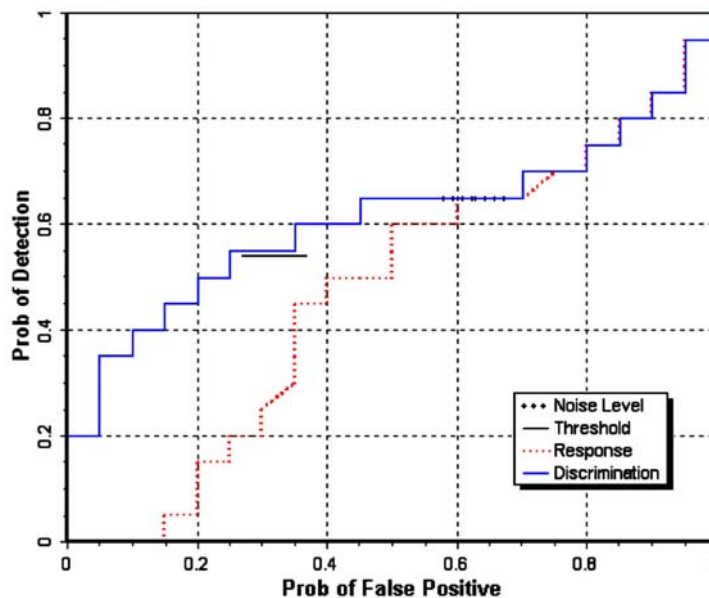


**Figure 14. EM61-HH ROC from Blind Grid Scoring Report [7]**

In Figure 14, the *Noise Level* line (black + signs) corresponds to a signal level of 40 mv. This is not the actual sensor noise level. It represents the signal level below which we did not bother to collect grid data. Our experience with the EM61-HH has been that targets with signal strength below this level are too weak to support classification and discrimination. The separation between the blue and red curves reflects how well we are discriminating between ordnance and clutter. For targets with signals greater than 40 mv (i.e., the portions of the curves below the noise level line) the blue curve is consistently above and to the left of the red curve. Here, we are correctly classifying targets significantly more often than not. Above the noise level line the two curves coincide, reflecting the fact that we made no attempt at discrimination for targets with

signal levels below 40 mv. The black *Threshold* line corresponds to a signal level of 60 mv. This is the level at which the discrimination *Efficiency* and the false positive *Rejection Rate* were evaluated.

The actual noise level in the data is a somewhat elusive quantity. We average data for about a second at each grid point on the template, and subtract a background level determined by interpolating between “blanks” taken off to the side of the grid before and after each set of template readings. For the data collected at the Standardized Test Site (Calibration Lanes plus Blind Grid), the number of samples that were averaged to produce sensor readings ranged between 2 and 34, with a median value of 7. Variations of the data about the sample means include contributions due to sensor noise and contributions arising from imperfect data collection. Median values of the standard deviations about the sample means are 0.30 mV, 0.22 mV, 0.15 mV and 0.12 mV for time gates 1 through 4, respectively. These values are indicative of the sensor noise level, which is then reduced by a factor of about  $\sqrt{7} = 2.6$  during the averaging process.

If the sensor is not held perfectly stationary during the sampling interval, then additional variation of the data about the sample mean is introduced because readings corresponding to different signal levels are being averaged together. During the demonstration this was not all that uncommon. Figure 15 shows data on the sampling statistics. On the left is a scatter plot of the first time gate sample mean vs. the sample standard deviation for all of the data from the Calibration Lanes and the Blind Grid. There is a big cloud centered on the median sample standard deviation of 0.30 mV and the median sample mean of 37.3 mV. At larger signal levels the sample standard deviation starts to increase, more or less in proportion to the sample mean. If internal receiver noise were the only factor causing signal variations, we would expect that the standard deviation would be independent of the mean. The observed trend indicates that this is not the case, and that slight motions of the sensor are introducing noise. The effect only appears when the signals become strong enough so that the motion-induced noise becomes larger than the receiver noise.

The right-hand plot in Figure 15 is a histogram of the ratio of sample standard deviation to sample mean for those data with signal levels greater than 200 mV and less than 10,000 mV (saturation level). The distribution is reasonably compact, centered on a median value of 0.0013. Most readings (~98%) have a sample standard deviation that is less than 1% of the sample mean. simple calculation reveals that a position error of 1 mm can cause a 1% signal error for a 25 cm deep target, and hence the sensor movement during the readings is actually less than 1 mm.

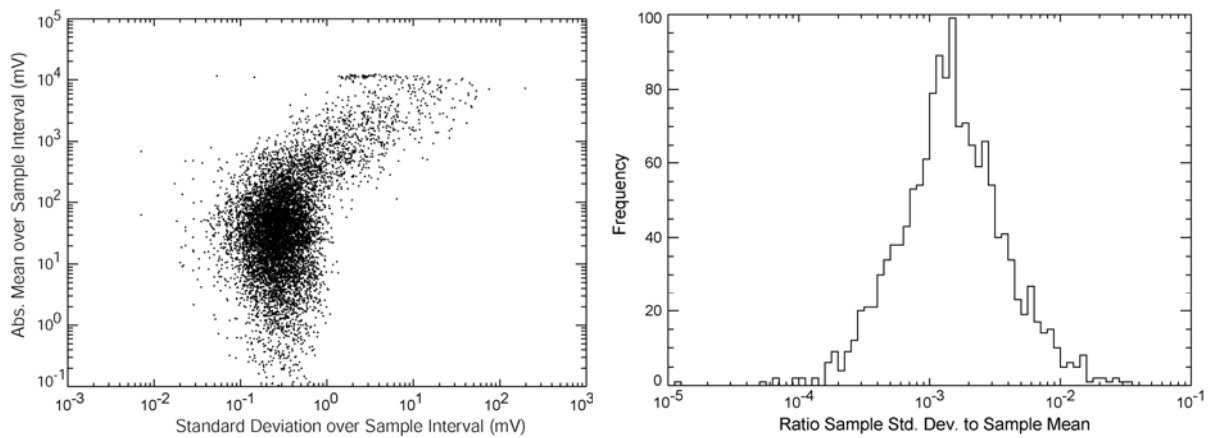


**Figure 15. Sample mean and standard deviation (left) and histogram of the ratio of sample standard deviation to sample mean for signal level >200 mV (right).**

The noise associated with removing the background level is summarized in Table 7. The column labeled Sensor Noise is the median value of the sample standard deviation. The last two columns summarize the statistics for the difference between background readings taken before and after the grid template readings. The mean (i.e. average over all the grids) background level difference is small. This simply says that there is no preferential bias, i.e. the background level before a grid is just as likely to be higher then the background level after the grid as lower. However, the last column in Table 7 shows that the differences in background level *are* significant. For first time gate data (the primary data source for inversion and target classification) the standard deviation of the difference between before grid and after grid background levels is ~7 mV. This is much larger than the sensor noise level, and probably comparable to the noise introduced by other vagaries of the data collection process.

**Table 7. Noise levels for EM61-HH grids.**

<b>Time Gate</b>	<b>Sensor Noise (mV)</b>	<b>Mean Background Difference (mV)</b>	<b>RMS Background Difference (mV)</b>
1	0.30	-0.02	7.06
2	0.22	0.14	2.33
3	0.15	0.06	1.15
4	0.12	0.05	0.63

For the most part, the dipole model does a good job of fitting the grid data. Figure 16 summarizes data on the performance of the dipole model fit. The plot on the left is a scatter plot of the RMS difference between the data and the dipole model fit to the data vs. mean signal level. It includes all of the grids from the Calibration Lanes and the Blind Grid with response

(peak signal) greater than 40 mV. The mean signal is taken over either an area defined by a circle with a radius equal to 1/2 times the apparent target depth, or the nine largest signal values, whichever includes more data points. We want to only include the actual anomaly in calculating the mean signal, without diluting it by including surrounding background points. However, for very shallow targets this area may not include enough data points. The inversion estimates nine parameters, so at least nine data points contribute significantly to fit process. On the right is a histogram of the ratio of the fit error to the mean signal. Usually, the dipole model can fit the data to within a few percent. The median value of the ratio of the dipole model fit error to the mean signal level is 0.024. (In terms of the peak signal level of the anomaly, the median ratio is 0.0077.) There are a fair number of targets for which the dipole response model does not do a good job. A few correspond to very weak signals, but others are strong anomalies. In many of these cases, it appears that there may be more than one target in the cell.

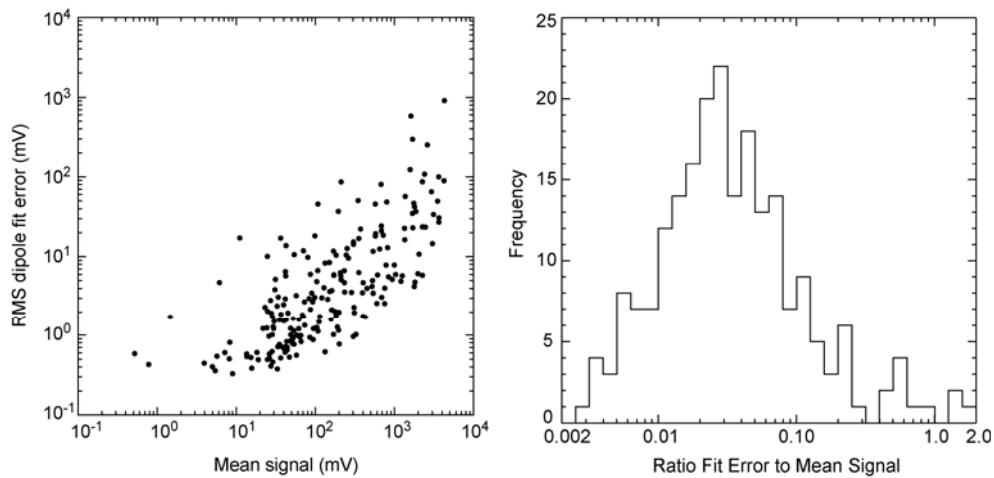


**Figure 16. Scatter plot of dipole model fit error vs. mean signal (left) and histogram of the ratio of fit error to signal level (right).**

## 5. Cost Assessment

### 5.1. Cost Reporting

The EM61-HH used in this demonstration was purchased from Geonics for \$17,295. It can be leased from Exploration Instruments for \$44 per day with a mobilization/demobilization fee of \$150. The cost of a grid template is negligible. All of the equipment can be easily transported in an automobile. Other than the capital cost or lease cost of the sensor, the major cost is labor.

A standardized estimate for Blind Grid demonstration labor costs is included in each Scoring Report. The cost was calculated as follows: the first person at the test site was designated

“supervisor”, the second person was designated “data analyst”, and the third and following personnel were considered “field support”. Standardized hourly labor rates were charged by title: supervisor at \$95.00/hour, data analyst at \$57.00/hour, and field support at \$28.50/hour.

Government representatives monitored on-site activity. All on-site activities were grouped into one of ten categories: initial setup/mobilization, daily setup/stop, calibration, collecting data, downtime due to break/lunch, downtime due to equipment failure, downtime due to equipment/data checks or maintenance, downtime due to weather, downtime due to demonstration site issue, or demobilization. See Appendix D of the Scoring Report for the daily activity log. See section 3.4 of the Scoring Report for a summary of field activities.

The standardized cost estimate associated with the labor needed to perform the field activities is presented in Table 10 of the Scoring Report [7], reproduced here as Table 8. Note that calibration time includes time spent in the Calibration Lanes as well as field calibrations. “Site survey time” includes daily setup/stop time, collecting data, breaks/lunch, downtime due to equipment/data checks or maintenance, downtime due to failure, and downtime due to weather.

**Table 8. Standardized Blind Grid Demonstration Labor Costs.**

	<b>No. People</b>	<b>Hourly Wage</b>	<b>Hours</b>	<b>Cost</b>
<b>Initial Setup</b>				
<b>Supervisor</b>	1	\$95.00	0.50	\$47.50
<b>Data Analyst</b>	0	57.00	0.00	0.00
<b>Field Support</b>	0	28.50	0.00	0.00
<b>Subtotal</b>				\$47.50
<b>Calibration</b>				
<b>Supervisor</b>	1	\$95.00	8.75	\$831.25
<b>Data Analyst</b>	0	57.00	0.00	0.00
<b>Field Support</b>	0	28.50	0.00	0.00
<b>Subtotal</b>				\$831.25
<b>Site Survey</b>				
<b>Supervisor</b>	1	\$95.00	18.33	\$1741.35
<b>Data Analyst</b>	0	57.00	0.00	0.00
<b>Field Support</b>	0	28.50	0.00	0.00
<b>Subtotal</b>				\$1741.35
<b>Demobilization</b>				
<b>Supervisor</b>	1	\$95.00	0.25	\$23.75
<b>Data Analyst</b>	0	57.00	0.00	0.00
<b>Field Support</b>	0	28.50	0.00	0.00
<b>Subtotal</b>				\$23.75
<b>Total</b>				\$2,643.85

## 5.2. Cost Analysis

Table 9 summarizes demonstration labor costs for all of the ATC Blind Grid demonstrations to date [6-14]. AETC is slightly less than the average Blind Grid demonstration cost of \$3,011.

**Table 9. Summary of ATC Blind Grid Labor Costs.**

<b>Demonstrator</b>	<b>Scoring Report</b>	<b>Cost</b>
<i>Zonge</i>	37	\$2,538.50
<i>AETC</i>	39	\$2,643.85
<i>Witten</i>	45	\$1,795.98
<i>Geophex</i>	49	\$3,772.64
<i>Geophex</i>	50	\$1,379.03
<i>Geophex</i>	125	\$2,354.29
<i>NRL</i>	127	\$1,640.65
<i>ERDC</i>	141	\$5,194.31
<i>ERDC</i>	142	\$2,890.47

The costs in Table 9 are calculated using a standard recipe for the test site that assumes standard rates for various labor categories. The actual AETC cost for the demonstration, including data analysis, was \$13,590. In addition to the data analysis cost, this reflects higher labor rates than shown in Table 8.

A more realistic figure for the cost of this technology can be obtained using the costs incurred in the field implementation at Bridgeport, Connecticut described in reference [5]. There, 694 targets were reacquired and interrogated by personnel from NAEVA Geophysics at a cost of \$45K, including mobilization and demobilization. The cost of data analysis and reporting by AETC personnel was \$35K. The net cost for doing cued interrogation in that operation was thus \$115 per target. Note that in the field, with targets scattered over a larger area, a production rate of about 30 targets per day is all that can be expected.

## 6. Implementation Issues

### 6.1. Environmental Checklist

We are not aware of any necessary permits or potential regulations that may apply to the demonstration. There are no emissions/residuals produced by the technology being demonstrated.

## 6.2. Other Regulatory Issues

The technology was described at the Interstate Technology Regulatory Council (ITRC) meeting in Monterey, California in September of 2003. It has been employed at a RCRA site in Bridgeport, Connecticut that is monitored by the EPA [5].

## 6.3. End-User Issues

The basic sensor (EM61-HH) is commercial, off the shelf technology. Data collection can be carried out by standard commercial geophysical survey crews. That has been demonstrated in the Bridgeport, Connecticut classification and discrimination work [5]. However, the processing and analysis procedures are not ready for general use. They require highly trained and motivated personnel for successful application. Furthermore, the demonstration results discussed in section 4 above indicate that at least in some cases, the detection efficiency may not be high enough for reliable UXO/clutter discrimination. Limitations on the use of the technology were discussed in section 2.4 above.

## 7. References

1. Bell, T. H., B. J. Barrow and J. T. Miller, 2001, *Subsurface Discrimination Using Electromagnetic Induction Sensors*, IEEE Transactions on Geoscience and Remote Sensing, Vol. 39, No 6., pp. 1286-1293.
2. Landau, L. D., and Lifshitz, E. M., 1960, *Electrodynamics of Continuous Media*, Pergamon Press, New York, pp. 186-193.
3. Baum, C. E. (Ed.), 1999, *Detection and Identification of Visually Obscured Targets*, Taylor and Francis, Philadelphia.
4. NAVEODTECHCEN, 1992, *Handheld Gradiometer Survey Test at The Marine Corps Air Ground Combat Center, Twentynine Palms, CA*, Technical Report, September.
5. Ambrose, Brian, Thomas Bell and Tom Furuya, 2004, *UXO Clearance at the Lake Success Redevelopment Project*, UXO/Countermine Forum, St. Louis, Missouri, March 9-12.
6. Overbay, Larry, 2003, *Standardized UXO Technology Demonstration Site Blind Grid Scoring Report No. 50*, U. S. Army Aberdeen Test Center Report ATC-8691, October 2003.
7. Overbay, Larry, 2003, *Standardized UXO Technology Demonstration Site Blind Grid Scoring Report No. 39*, U. S. Army Aberdeen Test Center Report ATC-8643, October 2003.
8. Overbay, Larry, 2003, *Standardized UXO Technology Demonstration Site Blind Grid Scoring Report No. 37*, U. S. Army Aberdeen Test Center Report ATC-8642, October 2003.
9. Overbay, Larry, 2003, *Standardized UXO Technology Demonstration Site Blind Grid Scoring Report No. 45*, U. S. Army Aberdeen Test Center Report ATC-8659, October 2003.

10. Overbay, Larry, 2003, *Standardized UXO Technology Demonstration Site Blind Grid Scoring Report No. 49*, U. S. Army Aberdeen Test Center Report ATC-86831, October 2003.
11. Overbay, Larry, 2003, *Standardized UXO Technology Demonstration Site Blind Grid Scoring Report No. 125*, U. S. Army Aberdeen Test Center Report ATC-8741, December 2003.
12. Overbay, Larry, 2004, *Standardized UXO Technology Demonstration Site Blind Grid Scoring Report No. 127*, U. S. Army Aberdeen Test Center Report ATC-8740, January 2004.
13. Overbay, Larry, 2004, *Standardized UXO Technology Demonstration Site Blind Grid Scoring Report No. 141*, U. S. Army Aberdeen Test Center Report ATC-8757, April 2004.
14. Overbay, Larry, 2004, *Standardized UXO Technology Demonstration Site Blind Grid Scoring Report No. 142*, U. S. Army Aberdeen Test Center Report ATC-8758, March 2004.

## 8. Points of Contact

**Table 10. Points of Contact**

<u>ESTCP</u>		
Jeffrey Marqusee	ESTCP Program Director	Arlington, VA
Anne Andrews	ESTCP Program Manager for UXO	Arlington, VA
Jeffrey Fairbanks	ESTCP UXO Program Coordination	Herndon, VA
<u>AETC</u>		
Thomas Bell	Demonstration Manager	Arlington, VA
<u>AEC</u>		
George Robitaille	AEC Demonstration Site Program Manager	Aberdeen Proving Ground, MD
<u>ATC</u>		
Larry Overbay	ATC Site Manager	Aberdeen Proving Ground, MD

**Dated Signature of Project Lead**

Thomas Bell  
AETC Incorporated

## Appendix A. Data Storage and Archiving Procedures

The raw sensor output data have been provided to ATC and the ESTCP Program Office for archiving. The IDL source code used in processing the data has also been provided to the ESTCP Program Office. The point of contact at ATC is Larry Overbay (see section 8 above). The files are in the standard Geonics DAT61 ASCII text format. A sample is shown in Figure 17. The first nine lines are header information. In the data section, column 1 is an event marker which will be used to identify readings at locations over the target, column 2 is the sequential reading number, columns 2-5 are sensor readings in mV for the four times gates (0.147, 0.263, 0.414, 0.613 msec), and the last column is the time of the reading in HH:MM:SS. For these data, the nominal data rate is 10 Hz, although the instrument actually delivers data at a slightly slower rate (readings arrive in 0.11 sec intervals). We have provided data logs which identify data file and line numbers with specific grids and specify the procedure to be used to relate specific readings with background levels and specific grid points.

```
=====EM61MK2 FILE HEADER=====
EM61MK2 V1.04 GRD 0 1 0
test2      0.100
          0.00      0.00      0.00      0.00
=====
L 2      test2      GRD 0 1 0
B          0.00 1
A E          1.000
Z 05/15/2002 12:27:59
E          0.00      103.87      113.64      27.28      -23.67 12:28:02.53
E          1.00      81.32      134.28      8.27      -0.65 12:28:02.64
E          2.00      76.87      21.08      4.79      42.47 12:28:02.75
E          3.00      100.91      -42.46      30.33      46.48 12:28:02.86
E          4.00      122.15      -11.66      45.43      1.41 12:28:02.97
E          5.00      121.24      104.19      43.83      -33.94 12:28:03.08
E          6.00      96.91      119.08      4.28      4.22 12:28:03.19
```

**Figure 17. Sample EM61 data file.**

The test stand signature data have also been provided to ATC for archiving. There is one text file for each grid above a target on the test stand. Each data file corresponds to EM61-HH signal measured on a 6x6 point square grid above the ordnance item. The format is comma delimited text. The first line identifies the ordnance type and orientation, e.g. 45 up is 45° dip with nose pointing up, flat X is 0° dip aligned along X axis, etc. Second line gives the column headings, the next 36 lines give X & Y coordinates of the measurements and the average EM61-HH signal at each of the four time gates. Background levels have been removed. Targets are located more or less at the center of the grid and at a depth that gives a reasonable signal level. Actual target X,Y locations and depths were not recorded.